An irregular feather-edge and potential outcrop of marine gas hydrate along the Mauritanian margin

Richard J. Davies[1], Jinxiu Yang[2,3], Ang Li[3], Simon Mathias[3] and Richard Hobbs[3]

[1]School of Civil Engineering and Geosciences, Newcastle University, Newcastle upon Tyne, Tyne and Wear, NE1 7RU, UK.

[2]Research Institute of Unconventional Oil & Gas and New Energy, China University of Petroleum (Huadong), No 66 Changjiang West Road, Huangdao District, Qingdao, Shandong, 266555, China.

[3]Centre for Research into Earth Energy Systems (CeREES), Department of Earth Sciences, Durham University, Science Labs, Durham DH1 3LE., UK.

Corresponding author email address: richard.davies@ncl.ac.uk

ABSTRACT

The dissociation of marine hydrate that surrounds continental margins is thought to be an agent for past and future climate change. As the water depth decreases landwards, the base of the hydrate stability zone progressively shallows until hydrate occurs immediately below the seabed where an increase in bottom water temperature can cause dissociation. But the true extent of these most vulnerable hydrate deposits is unknown. Here we use exceptional quality three-dimensional (3-D) seismic reflection imagery offshore of Mauritania that reveals a rare example of a bottom simulating reflection (BSR) that intersects the seabed and delineates the feather-edge of hydrate. The BSR intersects the seabed at the ~636 m isobath but along the 32 km of the margin analysed, the intersection is highly irregular. Intersections and seismic evidence for hydrate less than ~ 4.3 m below the seabed occur in seven small, localised areas that are 0.02 - 0.45 km^2 in extent. We propose gas flux below the dipping base of the hydrate to these places has been particularly effective. The intersections are separated by recessions in the BSR where it terminates below the seabed, seaward of the 636 m isobath. Recessions are areas where the concentration of hydrate is very low or hydrate is absent. They are regions that have been bypassed by gas that has migrated landward along the base of the hydrate or via hydraulic fractures that pass vertically through the hydrate stability zone and terminate at pockmarks at the seabed. An irregular feather-edge of marine hydrate may be typical of other margins.

Keywords: hydrate; seabed; dissociation; warming; reflection; gas

1. Introduction

Marine gas hydrate is a solid compound of water and gas that occurs in many settings, including sediment surrounding deep water continental margins. The stability of hydrate is related to temperature and pressure (P-T) and in these settings the progressive landward reduction in water depth causes the base of the gas hydrate stability zone (BHSZ) to shallow and intersect the seabed. This configuration results in a potential hydrate zone that thins in a landward direction (Dickens, 2001; Milkov and Sassen, 2000) that has been termed the feather-edge of marine hydrate (Fig. 1A; Ruppel, 2011).

The feather-edge holds ~3.5% (Ruppel, 2011) of the estimated ~$7x10^2$ - ~$1.27x10^4$ Gt of carbon held in marine hydrates (Dickens, 2011). Where the BHSZ intersects the seabed, hydrate may occur at the sediment-water interface (e.g. Egorov et al., 1999) or because of the anaerobic oxidation of the methane, just below it (Barnes and Goldberg, 1976). Past, rapid climate perturbations have been attributed to several different phenomena, including the dissociation of marine hydrate (Dickens et al., 1995). Warming of the seabed in the feather-edge domain could cause dissociation after only a few decades, because of the proximity of the hydrate to the seabed (Thatcher et al., 2013). Dissociation could even be seasonal (Berndt et al., 2014) or associated with changes in seabed temperature caused by upwelling currents (see Hagen, 2001). Methane release has been documented at the feather-edge of marine hydrate offshore of Svalbard (Westbrook et al., 2009; Berndt et al., 2014) and the eastern North American margin (Phrampus and Hornbach, 2012; Skarke et al., 2014).

Although hydrate dissociation has long been proposed as a mechanism for climate change (e.g. Dickens et al., 1995) and there is potential evidence for dissociation on some margins, descriptions of the feather-edge using seismic reflection data lack detail (Ben-Avraham et al., 2002; Coffin et al., 2011; Phrampus and Hornbach, 2012). This is because they are based upon widely spaced two-dimensional (2-D) seismic lines and there are no borehole calibrations. Key questions remain; for instance, regarding the amount of hydrate that is vulnerable, whether it occurs consistently along continental margins and how gas migrates to sustain it. Here we provide the first 3-D seismic description of the feather-edge of marine hydrate, based upon the mapping of a BSR that intersects the seabed. We describe the evidence for outcropping of hydrate and consider how gas sustains hydrate in these settings.

2. Hydrate and the Feather-Edge

In addition to P-T conditions, hydrate formation is controlled by the concentration of dissolved gas, which needs to be higher than its solubility in pore water (Xu and Ruppel, 1999). The BHSZ can coincide with the base of a hydrate accumulation, although this is not necessarily the case (Xu and Ruppel, 1999) and it may or may not be marked by a BSR (e.g. Dillon, et al., 1980).

BSRs in hydrate provinces, including this one, are recognized as high-amplitude, negative polarity reflections, usually caused by the velocity contrast between sediment partially saturated with hydrate above it and sediment partially saturated with free gas below it (Field and Kvenvolden, 1985). The minimum saturation of hydrate in sediment required to cause a moderate or significant increase in acoustic impedance is unclear. It could be as little as 2% (Helgerud et al., 1999), 14% (Hu et al., 2014) or in excess of 40% (Carcione and Tinivella, 2000). The saturation of hydrate within the hydrate stability zone can be highly variable, with the highest saturations often occurring in porous sands, permeable layers and faults (e.g. Malinverno et al., 2008). This heterogeneity may be one of several factors that determine how the hydrate manifests itself where it outcrops at seabed.

We define the feather-edge of gas hydrate, also referred to as the hydrate wedge (Gorman and Senger, 2010), as the region where the BHSZ starts to shallow and intersects the seabed because of a progressive landward reduction in water depth (Fig. 1A). Since hydrate formation and dissociation are closely linked to the ambient P-T conditions, the intersection should be at a consistent depth along the margin, often ~300 - 600 m (e.g. Milkov and Sassen, 2000). But this is also dependent on the composition of hydrocarbons in the hydrate with the shallower intersections occurring where methane is accompanied by other hydrocarbon gases (Milkov and Sassen, 2000). Seaward of the intersection, hydrate could exist at the seabed (e.g. Egorov et al., 1999; MacDonald et al., 1994) in an outcrop zone (Fig. 1A).

Evidence for the feather-edge of marine gas hydrate has been detected using 2-D seismic data for example on the margins of South Africa (Ben-Avraham et al., 2002 – e.g. their figure 2) and Chile (Coffin et al., 2011) the North Island of New Zealand (Crutchley et al., 2010). Off West Svalbard, there is evidence for a feather-edge on the basis of gas flares that occur only landward of the 396 m isobath (Chabert et al., 2011; Sarker et al., 2012; Westbrook et al., 2009). In the northwest Black Sea, Naudts et al. (2006) described gas plumes that occur landward of the 725 m isobath and similar observations are also made off the northern US Atlantic margin (Skarke et al., 2014).

In terms of how gas migrates to the landward limit of marine hydrate, at the West Svalbard feather-edge, Thatcher et al. (2013) proposed that gas migrates vertically through fractures toward the BHSZ; laterally within seaward-dipping permeable strata or along the base of the hydrate. At this feather-edge, carbonates at gas seeps indicate venting has been occurring for > 3000 yrs. (Berndt et al., (2014). Large-scale 2-D modelling of the feather-edge on this margin shows that warming could cause methane release near the landward limit of the top of the hydrate stability zone (Reagan and Moridis, 2009).

3. Seismic Data and Geological Setting

The offshore Mauritania 3-D seismic survey was processed by several steps including multiple suppression and post-stack time migration. The dominant frequency of this data at the depth of the hydrate is ~50 Hz. The typical seismic velocity at the depth of investigation is ~1700 ms^{-1} and therefore 100 milliseconds two-way-travel time (ms TWT) on seismic sections is equivalent to approximately 85 m. The final bin spacing of the seismic grid is 25 × 25 m. The data are minimum phase and a negative acoustic impedance contrast is represented as a black-red (negative polarity) reflection. Amplitude maps are all root mean square (RMS – see Brown, 2010) on the reflection itself, rather than over a time window.

In the study area the seabed dips at ~1° (Fig. 1B) and the BSR generally dips at an angle of ~2.3°. This increases as it shallows from 200 mbsf (meters below seafloor) to intersect the seabed at a seabed intersection depth (SID) of 636 m (Fig. 1C). We have not identified evidence for an opal-A to opal-CT diagenetic BSR in the dataset, which can occur at similar depths below seabed, but in contrast gives rise to a red-black reflection (trough-peak, positive polarity) reflection (see Davies and Cartwright, 2002). Below the BSR, at least

368 vertical seismic chimneys (e.g. Fig. 2A) are observed in the data by Davies and Clarke (2010) and interpreted as networks of hydraulic fractures that allow for the vertical migration of pore fluid and gas. Most of the chimneys terminate at or below the BSR.

The margin has several proven oil and gas accumulations and we do not have data on the gas composition of the hydrate. Hydrocarbon exploration wells in the area of the 3D seismic data (Chinguetti V1 and Chinguetti-6-1 – Fig. 1B) show that the sediment hosting the hydrate and the BSR probably span the last 5.2 Ma (Vear, 2005) and scientific drilling 150 km to the north (Henrich et al., 2010) indicates that in a similar setting fine-grained turbidites and foram-nannofossil hemipelagites were deposited. Industry geotechnical data from an area 100 km to the south, acquired at similar water depths, provides additional information on the seabed temperature (Lane, 2005). Measurement of water temperature at a 500 m water depth shows a mean temperature variation of 9.6 ºC to 10.5 ºC, over the five month period between August and December 2002. Lane (2005) also reports the measured sediment temperatures at four sites between 539 - 800 m were cooler than the water column at equivalent depths. An upwelling undercurrent fed by South Atlantic Cold Water (SACW) feeds a belt of upwelling along the margin (Hagen, 2001).

4. Description of the BSR

4.1 Bands of High Seismic Amplitude at the BSR

The general shape of the BSR is revealed by contours of its depth below sea level superimposed on the RMS seismic amplitude map of the reflection and shows that it has a curved (concave downward) form that shallows landward (Fig. 1C). The map reveals continuous and semi-continuous bands of high seismic amplitude that are 0.5 – 1.5 km wide and up to 30 km in length. Here we analyse two examples (areas marked by white boxes in Fig. 1C) which have variable geometries and orientations relative to the strike of the BSR (Fig. 1B and C). Most of the bands terminate without reaching the 636 m isobath (Fig. 1C).

The first example (Fig. 2C) consists of nine high-amplitude bands (marked I to IX - Fig. 2AB). They are east-west and southwest-northeast orientated (Fig. 2AB). A representative seismic cross section shows that they are negative-polarity reflections (the opposite to the seabed reflection) and occur immediately down-dip from where these reflections intersect the BSR. The intersections are coincident with possible phase reversals (Fig. 2B inset). The differential relief for an individual band is up to 600 m, although they may not be continuous and connected along their entire length (Fig. 2A).

In the second example a single band of high seismic amplitude is up to 2 km wide and 12 km long (Fig. 3AB). Again it corresponds to a negative polarity reflection at the interpreted level of the BSR (Fig. 3AB). The northern boundary to the band is a line of intersection (see Davies et al., 2012) that marks where the high-amplitude reflection intersects the BSR (marked by the yellow dot in Fig. 3B). The BSR is also characterised by regions where there are no distinctive bands of high seismic amplitude (Fig. 1C). These areas occur where there is concordance between the BSR and stratal reflections or where reflections have been disrupted due to slope processes (e.g. slope failure outlined in Fig. 1C).

4.2 Steps in the BSR

The BSR shallows either gradually or in a series of steps (Fig. 4A-D). The steps are regions where the BSR is locally concordant with stratal reflections. They are separated by narrower regions where the BSR cross-cuts them (Fig. 4). The steps are 0.5 - 3 km wide and up to 9 km long. The shallowest one (marked step 1 in Fig. 4B) occurs where the negative polarity BSR reflection is immediately below the seabed reflection (positive polarity). Step 1 does not extend along the entirety of the feather-edge but occurs locally in 5 places (encircled by dashed black lines - Fig. 4A). A seismic line that transects two of these areas (Fig. 4C) shows that there are clear gaps in the BSR reflection with the lateral terminations of the BSR being marked by phase reversals (marked by yellow circles in Fig. 4C).

We predicted the position of the BHSZ at steady state by using the hydrate stability curve for pure methane given by Moridis (2003) with a correction for sea water salinity of 35 wt% (see methodology of Davies et al., 2012). The stepped geometry of the BSR approximately follows the curved form predicted for the BHSZ (blue dashed line in Fig. 4D; see Gorman and Senger, 2010).

4.3 Intersection of the BSR with the Seabed

We mapped the intersections along 32 km of the margin. The landward extent of the BSR is highly irregular and there is no continuous intersection between the BSR and the seabed. Instead intersections occur over very restricted sections of the seabed along the 636 m isobath (Fig. 4A and B). Between these intersections there are gaps in the BSR (herein termed recessions - see Figs 1, 3-6) where it terminates below rather than at the seabed. In these localities there are no anomalous high-amplitude reflections that could be indicative of increased acoustic impedance, which would be consistent with high hydrate saturations (Carcione and Tinivella, 2000).

Approximately circular pockmarks occur on the seabed where there are recessions in the BSR and in some places, landward of the SID (marked with red and black circles and labelled 1, 2 and 3 on Fig. 5BC). In contrast there are no circular features of this kind on the seabed above the mapped BSR (Fig. 5A). They are 100 - 400 m wide. Below the seabed pockmarks are vertical seismic chimneys that extend for 300 - 600 m (marked by black arrows – Fig. 5C). Some of the bases of these chimneys emanate from high-amplitude reflections (Fig. 5ABC). The seabed dip map (Fig. 5A) has an uneven relief above the mapped BSR.

Similar observations of pockmarks immediately landward of the feather-edge, based upon bathymetry data acquired in 2003, have been made 100 km to the South of this study area (Lane, 2005). They are 60 - 800 m in diameter and occur within a north – south orientated area between the 540 – 640 m isobath. Hard calcareous accretions, which may represent authigenic carbonates, were recovered from a shallow core from one of the pockmarks (Lane, 2005).

Step 1 is the shallowest of the four steps and is immediately below the seabed. It is not perfectly concordant with stratal reflections. Instead, the BSR reflection shallows gradually in a landward direction (Fig. 6B) until, at its eastern end, there is a reduction in the amplitude of the seabed reflection (Fig. 6C). This is coincident with doming of the seabed reflection. Similar changes in reflection amplitude are detected in six other places along the 636 m isobath on an RMS amplitude map of the seabed (Fig. 6A). On seismic sections, the seabed and BSR interfaces should still be resolved when the distance between them is ~1/4 of the seismic wavelength. At ~1/8 of the wavelength the interference of the two reflections will cause a reduction in seismic amplitude (see Widness, 1973). Using a sediment velocity of 1700 ms^{-1} and a frequency of the seismic data of 50 Hz, we estimate 1/8 of the wavelength to be a distance of ~4.25 m (see Widness, 1973). Therefore, the hydrate-gas interface is ~4.25 m below the seabed. The seven places on the eastern margin of step 1 where these characteristics are observed have areas of between 0.02 - 0.45 km^2 (Fig. 6B).

5. Interpretation

5.1 High-amplitudes at the BSR

The bands of relatively high seismic amplitude are negative polarity reflections which is the opposite polarity to the seabed reflection (e.g. Fig. 3B). Phase reversals are also coincident with the intersections of these reflections with the BSR (Fig. 2B). As the bands occur at the BSR, their amplitude depends on the velocity and density of the hydrate and sub-hydrate sediment. A strong negative polarity reflection is probably caused by the transition from hydrate-saturated sediment to sediment containing some free gas as this would create the necessary decrease in acoustic impedance (Domenico, 1977; Carcione and Tinivella, 2000). When taken together, the observations are consistent with the bands of high seismic amplitude representing free gas that is sealed by hydrate-saturated sediment at the BSR (e.g. Chabert et al., 2011).

Davies et al. (2012) proposed that the bands form as a result of upward resetting of the BHSZ, driven by sedimentation, which leads to the dissociation of hydrate. The characteristic width of 0.5 to 3 km is therefore related to the angle of the intersection and the magnitude of the last upward shift in the BHSZ (i.e. narrow bands would form where there is a high angle of intersection and a small upward shift in the BHSZ). Although the bands appear on the amplitude maps to have a vertical relief of up to ~600 m (e.g. band XII – Fig. 2A), they are unlikely to represent fully interconnected reservoirs of free gas as the pore pressure at the shallowest terminations would exceed lithostatic pressure (Davies and Clarke, 2010 - their figure 4).

In fine-grained sediments, horizontal permeability is often several times that of the vertical permeability (e.g. Ayan et al., 1994; Yang and Aplin, 2007). Where the bands are parallel to the dip of the BSR, the configuration provides relatively high permeability migration routes for gas sealed below the hydrate-saturated sediment. When they are parallel to the strike of the BSR, the configuration is less conducive for up-dip migration of gas below the BSR. Disruptions in bedding, caused by slope failures would also impede up-dip migration of gas (Fig. 1C).

The vertical seismic chimneys (Fig. 2A) are generally interpreted to be evidence for clusters of hydraulic fractures (Zuhlsdorff and Spieß, 2004), suggesting vertical migration of gas has occurred to the base of the feather-edge of the hydrate, as predicted elsewhere (Thatcher et al., 2013; Westbrook et al., 2009).

5.2 *Variable Extent of Feather-Edge*

The map of the BSR reveals recessions where the BSR does not intersect the seabed. In these recessional areas, the negative polarity BSR switches abruptly to a positive polarity reflection (Fig. 4C). These areas could be where hydrate saturations are high enough to provide an effective seal for free gas, but no free gas is present. This could be because gas has not migrated to these localities, or is present but not in high enough saturations to exceed the solubility of methane in pore water (Xu and Ruppel, 1999; Haacke et al., 2007). Alternatively concentrations of hydrate could be too low to provide an effective seal for free gas. It is also plausible that the vertical clusters of hydraulic fractures allow gas to bypass the hydrate stability zone.

Seabed venting of free gas has sometimes been a proxy for the landward extent of hydrate at the feather-edge (Naudts et al., 2006; Westbrook et al., 2009). Although gas chimneys often penetrate hydrates (Wood et al., 2002) and reach the seabed (Liu and Flemings 2006), in this dataset, the occurrence of chimneys that penetrate the BSR are rare (Davies and Clarke, 2010) and we do not detect any seabed pockmarks above the BSR. 100 km to the south, pockmarks only occur landward of the 640 m isobath (Lane, 2005) and landward of the 636 m isobath in this survey. This is where hydrate in the sediment is absent. Therefore our preferred interpretation of the recessions is that they are areas where hydrate concentrations are low enough for there to be no effective seal for free gas, so no BSR is imaged and venting via pockmarks occurs.

5.3 Seismically Imaged Outcrop Zone

The steps are strata-parallel and approximately follow the predicted position of the BHSZ (Fig. 4D). This is consistent with sediment properties being a major factor controlling the distribution of gas hydrates and therefore also the free gas sealed by the hydrate in the sediment. For instance, hydrate concentrations tend to be higher in coarse-grained, more porous sediments (Malinverno, 2010; Weinberger et al., 2005), which would provide a more effective seal for free gas. We interpret steps to form because hydrate concentrations are higher in more porous strata. We are unclear as to why it should occur in one part of the survey and not throughout it.

At the landward end of step 1 the characteristic positive polarity seabed reflection is located immediately above the negative polarity BSR reflection (Fig. 6B). The change in reflection character of the seabed (Fig. 6C) is probably due to tuning of the two reflections. When the thickness between the seawater-seabed interface and hydrate-free gas interface is less than ~1/4 of the wavelength $\lambda/4$ (~8.5 m), two reflections will no longer be resolved. When the thickness is ~1/8 of the wavelength, the amplitude of the seabed reflection should decrease as a result of destructive interference between the reflections from the two interfaces (Widness, 1973). Where we observe a drop in amplitude (Fig. 6C) we predict that in these locations free gas is ponding only ~1/8 of the wavelength (~4.3 m) below the seabed and the hydrate can be no thicker than this. The slight mounding of the seabed coincident with the drop in amplitude (Fig. 6C) would be consistent with hydrate occurring at the seabed itself. Alternatively the response is related to carbonates at the seabed, but one would expect there to be an increase in seabed amplitude rather than a reduction. However, without direct evidence, such as video footage or drop cores we cannot be certain that there is hydrate at the sediment-water interface and hence term this a ‘seismically defined’ outcrop zone.

6. Discussion

6.1 Gas Migration to the Feather-Edge

The observations support several mechanisms by which gas migrates to the feather-edge. Advection through hydraulic fractures which are manifested as vertical seismic chimneys (Zuhlsdorff and Spieß, 2004) is one mechanism (Davies and Clarke, 2010; Davies et al., in review). Gas could either be incorporated into the hydrate or pond below the hydrate, if the pore fluid is super saturated with respect to gas (Haacke et al., 2007). We propose some gas migrates along the base of the hydrate and that this occurs dominantly within regularly-spaced, relatively high permeability beds that intersect the BSR. Where lines of intersection are parallel to the dip of the seabed and BSR they are orientated favourably for gas migration to the feather-edge of the hydrate. Gas could also migrate along the base without being confined to these higher permeability channels, by diffusive flow. The gently curved (concave downward) and dipping geometry of the BSR, creates a natural focus for gas migrating along its base, towards the few places where a BSR does intersect the seabed (Fig. 1C).

6.2 Dissociation of the Feather-Edge

The seven areas where we interpret hydrate to be located within 4.3 m of the seabed are ~0.02 to ~0.45 km^2 in area. Collectively, they represent an area of 0.85 km^2 (Fig. 6A). Given that the hydrate is ≤ 4.3 m in thickness across these regions the maximum volume of sediment containing hydrate at or immediately below the seabed (within 4.3 m) is ~0.0037 km^3. If step 1 existed along the entire study area (32 km in length) and the outcrop zone is 200 m wide and the hydrate is 4.3 m thick, then the total volume of sediment saturated with hydrate would be 0.0275 km^3. However, because outcrop zones are localised, the volume of hydrate-saturated sediment at or immediately below the seabed is a small fraction of this (0.0037 km^3). If warming of ocean currents occurs in the future, the time taken for thermal diffusion, hydrate dissociation, and gas migration, could be only a matter of decades (Thatcher et al., 2013), but because the outcrop zones are so localised the initial volumes of gas released would be modest initially and increase as deeper, more continuous areas of the hydrate were effected. The role that upwelling of cold water fed by the SACW could have in changing seabed temperature and therefore the stability of hydrate remains a key question.

7. Conclusions

The feather-edge of marine hydrate is rarely observed. In this example, the landward extent of the feather-edge of marine gas hydrate is irregular. Hydrate occurs at the seabed or immediately below it in very small, localised areas immediately seaward of the 636 m isobath. Hydrate is probably sustained here by migration of gas within favourably orientated relatively high permeability strata sealed by the overlying hydrate. An irregular feather-edge of marine hydrate may be typical of other margins.

Acknowledgements

The Landmark University Grant Program is gratefully acknowledged for providing seismic interpretation software. Dave Stevenson and Gary Wilkinson (Durham University) are acknowledged for managing the seismic interpretation facility and Petronas and Tullow Oil for permission to use the seismic reflection data. We thank Cristian Berndt for discussions. We thank Ingo Pecher and two anonymous reviewers for their very helpful comments.

FIGURE CAPTIONS

Figure 1 A: Schematic of the feather-edge region and outcrop zone, showing positions of three hypothetical BSRs (1, 2 and 3) shifting as a response to warming of the seabed. SID – seabed intersection depth and PoI – point of intersection (in this and subsequent figures). Inset – schematic graph of temperature (T) against depth (D) for when the BSR is located at position 3, showing the hydrate stability curve (HSC) and temperature curve (TC). SB – seabed and OZ – outcrop zone on this and subsequent figures. B: Map of the seabed in metres, imaged by the 3-D seismic dataset. Inset – location map for the study area. C: RMS seismic amplitude map of the BSR showing bands of high seismic amplitude and localised intersections of the BSR with the seabed at the SID. Dashed yellow lines – depth contours for the BSR relative to sea level.

Figure 2 A: RMS amplitude map of the BSR showing high-amplitude bands (I-IX). LoI – line of intersection (in this and subsequent figures). B: Seismic line across high-amplitude bands showing they occur at the intersection of stratal reflections with the BSR. Red dashed line in this and subsequent figures – BSR.

Figure 3 A: Representative seismic line A-A’ along a band of high seismic amplitude that intersects the BSR. Arrows mark the location of the BSR. Vertical full black line marks the change in orientation of the seismic line. Vertical black dashed line marks the intersection with line B-B’. Inset – 3-D schematic representation of high-amplitude bands at the BSR. B: Seismic line B-B’ across a band of high seismic amplitude. Vertical black dashed line marks the intersection of seismic line A-A’. Dashed white lines – high-amplitude bands located at and below the BSR. Inset – RMS amplitude map showing the location of lines A-A’ and B-B’. Red dashed line – interpreted position of the BSR. Black, white, yellow and red dots in

A and B mark the extent of the high-amplitude band in map view and seismic cross section. Small insets – contrasting reflection character between the positive polarity and negative polarity seabed and BSR reflections.

Figure 4 A. RMS seismic amplitude map of the BSR in the area where it intersects the seabed. Outlined regions correspond to steps in the BSR. Areas encircled with black dotted line – seven locations where step 1 identified. B: Representative seismic line (B-B') across the feather-edge of the hydrate. C: Representative seismic line (C-C') across the hydrate. Yellow circles mark phase reversals. SB – seabed; FG – free gas; GH – gas hydrate; AB – acoustic blanking. D: Seismic line B-B' showing the modelled and interpreted BSR intersecting the seabed.

Figure 5 Dip magnitude map of the seabed. Grey colours correspond to 1° dip, with lighter and darker shades representing very small changes in dip. White line – landward extent of the BSR. Red circles – pockmarks in the seabed. B: Zoom-in of part of the map in A. Yellow and black dots – lateral extent of the BSR with corresponding locations marked the representative seismic in C. Red circles – pockmarks (marked 1, 2 and 3). C: Representative seismic line across a recession in the BSR. Black arrows – vertical seismic chimneys. Black circles marked 1, 2, and 3 – three seabed pockmarks that correspond to those marked on B.

Figure 6 A: RMS amplitude map of the seabed. Dashed white line – the landward extent of the BSR. Orange area – places where there is evidence for a reduction in seismic amplitude of the seabed reflection consistent with hydrate immediate below or at seabed. Inset - seismic line A-A' across the SID.

REFERENCES CITED

Ayan, C., Colley, N., Cowan, G., Ezekwe, E., Wannell, M., Goode, P., Halford, F., Joseph, J., Mongini, A., Pop, J. 1994. Measuring permeability anisotropy: The latest approach: Oilfield Review, 6, 24-35.

Barnes, R.O., Goldberg, E.D., 1976. Methane production and consumption in anoxic marine sediments. Geology 4, 297-300.

Ben-Avraham, Z., Smith, G., Reshef, M., Jungslager, E., 2002. Gas hydrate and mud volcanoes on the southwest African continental margin off South Africa. Geology, 30, 927-930.

Berndt, C., Feseker, T., Treude, T., Krastel, S., Liebetrau, V., Niemann, H., Bertics, V. J., Dumke, I., Dünnbier, K., Ferré, B., Graves, C., Gross, F., Hissmann, K., Hühnerbach, V., Krause, S., Lieser, K., Schauer, J., Steinle, L., 2014. Temporal Constraints on Hydrate Controlled Methane Seepage off Svalbard, Science, 343, 284-287.

Brown, A., 2010. Interpretation of Three-Dimensional Seismic Data, seventh edition: Tulsa.

Carcione, J.M., Tinivella, U., 2000. Bottom-simulating reflectors: Seismic velocities and AVO effects, Geophysics, 65, 54-67.

Chabert, A., Minshull, T.A., Westbrook, G.K., Berndt, C., Thatcher, K.E., Sarkar, S., 2011. Seismic characterisation of gas hydrate and free gas along the western continental margin of Svalbard, Journal of Geophysical Research, 116, B12102.

Coffin, R., Pohlman, J., Gardner, J., Downer, R., Wood, W., Hamdan, L., Walker, S., Plummer, R., Gettrust, J., Diaz, J., 2007. Methane hydrate exploration on the mid Chilean coast: A geochemical and geophysical survey, Journal of Petroleum Science and Engineering, 56, 32–41.

Crutchley, G. J., Geiger, S., Pecher, I.A., Gorman, A. R., Zhu, H., Henrys, S. A., 2010. The potential influence of shallow gas and gas hydrates on seafloor erosion of Rock Garden, an uplifted ridge offshore of New Zealand, Geo-Marine Letters, 30, 283–303.

Davies, R.J., Cartwright, J.A. 2002. A fossilised Opal A to C/T transformation on the northeast Atlantic margin. Basin Research, 14, 467-486.

Davies, R.J., Clarke, A.L., 2010. Methane recycling between hydrate and critically pressured stratigraphic traps, offshore Mauritania, Geology, 38, 963–966.

Davies, R.J., Thatcher, K. E., Armstrong, H., Yang, J., Hunter, S., 2012. Tracking the relict bases of marine methane hydrates using their intersections with stratigraphic reflections. Geology, 40, 1011-1014.

Davies, R.J., Yang, J. Hobbs, R, Li, A., 2014. Probable patterns of gas flow and hydrate accretion at the base of the hydrate stability zone, Geology, 42, 1055-1058.

Dickens, G., O'Neil, J.R., Rea, D.K., and Owen, R.M., 1995. Dissociation of oceanic methane hydrate as a cause of the carbon isotope excursion at the end of the Paleocene. Paleoceanography, 10, 965–971.

Dickens, G.R., 2001. The potential volume of oceanic methane hydrates with variable external conditions. Org. Geochem. 32, 1179–1193.

Dickens, G.R., 2011. Down the rabbit hole: Toward appropriate discussion of methane release from gas hydrate systems during the Paleocene-Eocene thermal maximum and other past hyperthermal events. Climate of the Past, 7, 831-846.

Dillon, W.P.J., Grow, J.A., Paull, C.K., 1980. Unconventional gas hydrate seals may trap gas off southeast U.S. Oil & Gas Journal, 78, 124–130.

Domenico, S.N., 1977. Elastic properties of unconsolidated porous sand reservoirs, Geophysics, 42, 1339–1368.

Egorov, A.V., Crane, K., Vogt, P.R., Rozhkov, A.N., 1999. Gas hydrates that outcrop on the sea floor: stability models. Geo-Marine Letters, 19, 68-75.

Field, M.E., Kvenvolden, K.A., 1985. Gas hydrates on the northern California continental margin. Geology, 13, 517-520.

Haacke, R.R., Westbrook, G.K., Hyndman, R.D., 2007. Gas hydrate, fluid flow and free gas: Formation of the bottom-simulating reflector. Earth and Planetary Science Letters, 261, 407-420.

Hagen, E., 2001. Northwest African upwelling scenario, Oceanologica Acta, 24, S113–S128.

Henrich, R., Cherubini Y., Meggers H., 2010. Climate and sea level induced turbidite activity in a canyon system offshore the hyperarid Western Sahara (Mauritania): The Timiris Canyon. Marine Geology. 275, 178-198.

Hu G., Ye, Y., Zhang, J., Liu, C., Li Q., 2014. Acoustic response of gas hydrate formation in sediments from South China Sea. Marine and Petroleum Geology, 52, 1–8.

Gorman, A. R., Senger, K., 2010. Defining the updip extent of the gas hydrate stability zone on continental margins with low geothermal gradients. Journal of Geophysical Research v. 115, B07105.

Lane A., 2005. Overcoming Deepwater Geohazards in West Africa, OTC 17496.

Liu, X., Flemings, P.B., 2006. Passing gas through the hydrate stability zone at southern Hydrate Ridge, offshore Oregon: Earth and Planetary Science Letters, 241, 211-226.

MacDonald, I.R., Guinasso, N.L., Jr., Sassen, R., Brooks, J.M., Lee, L., Scott, K.T., 1994. Gas hydrate that breaches the sea floor on the continental slope of the Gulf of Mexico: Geology, 22, 699-702.

Malinverno, A., Kastner, M., Torres, M. E., Wortmann. U. G., 2008. Gas hydrate occurrence from pore water chlorinity and downhole logs in a transect across the northern Cascadia margin (Integrated Ocean Drilling Program Expedition 311), Journal of Geophysical Research, 113, B08103.

Malinverno, A., 2010. Marine gas hydrates in thin sand layers that soak up microbial methane: Earth and Planetary Science Letters, 292, 399-408.

Milkov, A.V., Sassen, R., 2000. Thickness of the gas hydrate stability zone, Gulf of Mexico continental slope, Marine and Petroleum Geology 17, 981–991.

Moridis, G.J., 2003. Numerical studies of gas production from methane hydrates: Society of Petroleum Engineers Journal. 32, 359-370.

Naudts, L., Greinert, J., Artemov, Y, Staelens P, Poort J, Van Rensbergen, P., De Batist, M., 2006. Geological and morphological setting of 2778 methane seeps in the Dnepr paleo-delta, northwestern Black Sea: Marine Geology, 227, 177– 199.

Phrampus, B. J., Hornbach, M. J., 2012. Recent changes to the Gulf Stream causing widespread gas hydrate destabilization, Nature, 490, 527–530.

Reagan, M. T., Moridis, G. J., 2009. Large-scale simulation of methane hydrate dissociation along the West Spitsbergen Margin, Geophysical Research Letters, 36, L23612.

Ruppel, C. D., 2011. Methane hydrates and contemporary climate change Nature Education Knowledge, 2(12):12.

Sarkar, S., Berndt, C., Minshull, T.A., Westbrook, G.K., Klaeschen, D., Masson, D., Chabert, A., Thatcher, K.E., 2012. Seismic evidence for shallow gas-escape features associated with a retreating gas hydrate zone offshore west Svalbard, Journal of Geophysical Research, 117, B09102.

Skarke, A., Ruppel, C., Kodis, M., Brothers, D., Lobecker, E., 2014. Widespread methane leakage from the sea floor on the northern US Atlantic margin. Nature Geoscience, 7, 657-661.

Thatcher, K. E., Westbrook, G. K., Sarkar, S., Minshull, T. A., 2013. Methane release from warming-induced hydrate dissociation in the West Svalbard continental margin: Timing, rates, and geological controls, Journal of Geophysical Research: Solid Earth, 118, 22–38.

Vear, A., 2005. Deep-water plays of the Mauritanian continental margin. In *Petroleum Geology: North-West Europe and Global Perspectives – Proceedings of the 6th Petroleum Geology Conference* (Eds Doré A.G. and Vining B. A.) (The Geological Society London), 1217-1232.

Weinberger, J.L., Brown, K.M., Long, P.E., 2005. Painting a picture of gas hydrate distribution with thermal images: Geophysical Research Letters, 32, L04609.

Westbrook, G.K., (and 18 co-authors) 2009. Escape of methane gas from the seabed along the West Spitsbergen continental margin: Geophysical Research Letters. 36, L15608.

Widness, M., 1973. How thin is a thin bed? Geophysics, 38, 1176-1180.

Wood, W.T., Gettrust, J.F., Chapman, N.R., Spence, G.D., Hyndman, R.D., 2002. Decreased stability of methane hydrates in marine sediments owing to phase-boundary roughness: Nature, 420, 656–660.

Xu, W., Ruppel, C., 1999. Predicting the occurrence, distribution, and evolution of methane gas hydrate in porous marine sediments, Journal of Geophysical Research: Solid Earth 104, 2156-2202.

Yang Y., Aplin, A.C., 2007. Permeability and petrophysical properties of 30 natural mudstones. Journal of Geophysical Research 112, B03206.

Zuhlsdorff, L., Spieß, V., 2004. Three-dimensional seismic characterization of a venting site reveals compelling indications of natural hydraulic fracturing, Geology, 32, 101–104.

Highlights:

- We provide the first description of the feather-edge of marine hydrate using three-dimensional seismic data.
- The landward extent of it, offshore of Mauritania is irregular and this may be typical for other margins.
- Hydrate that occurs at or below the seabed is rare along the margin.

Figure

Click here to download high resolution image

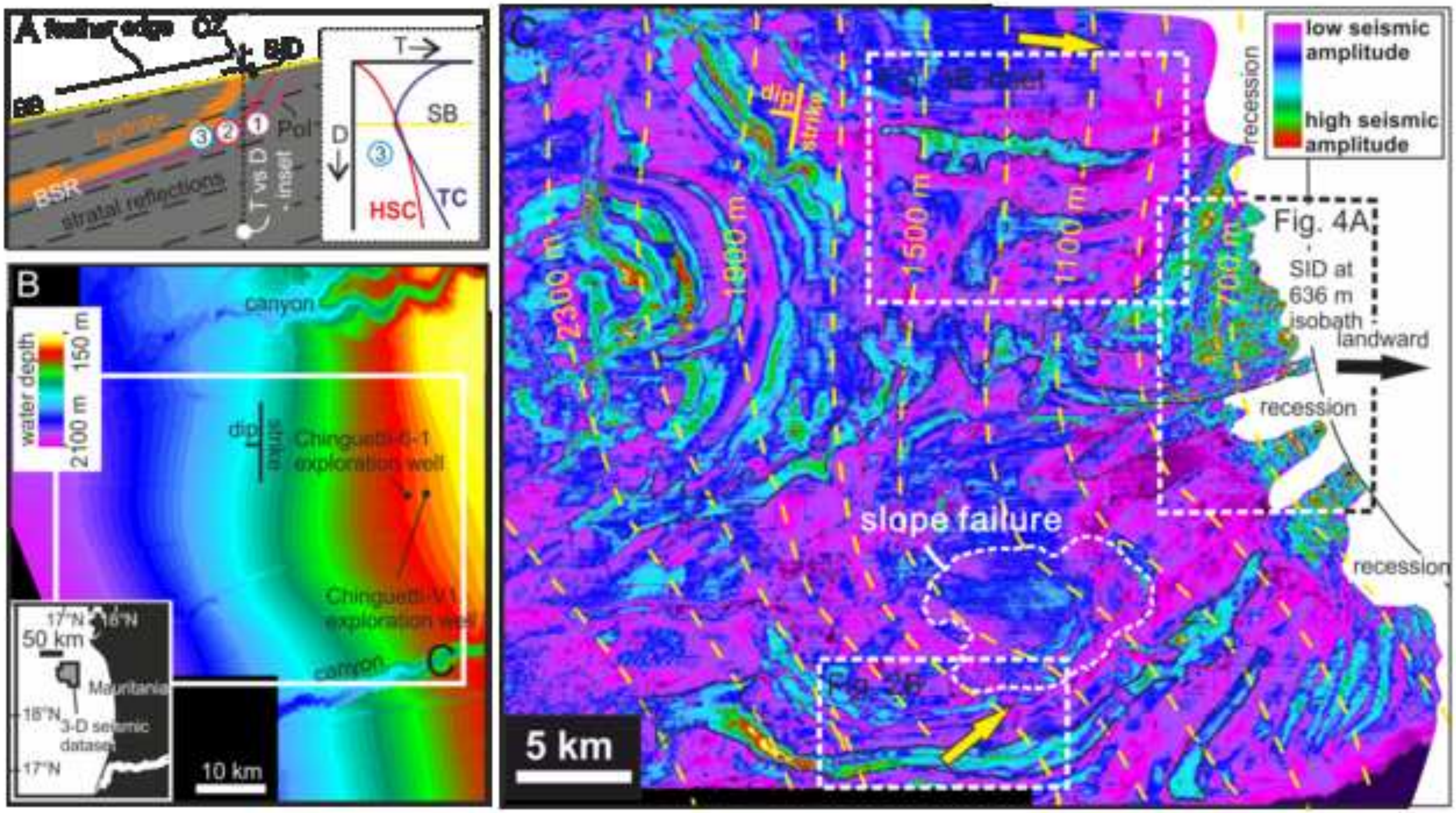

Figure
Click here to download high resolution image

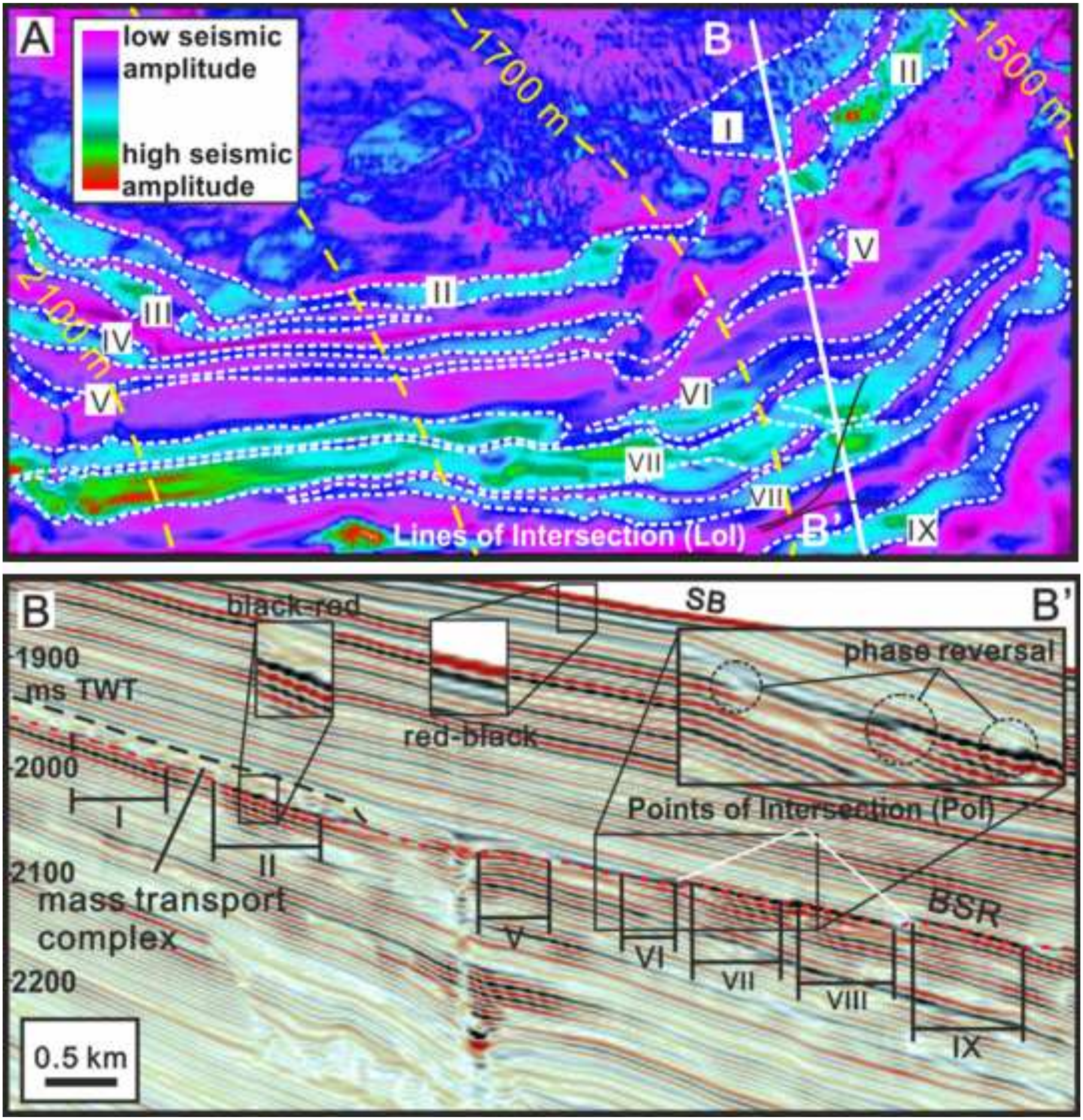

Figure
Click here to download high resolution image

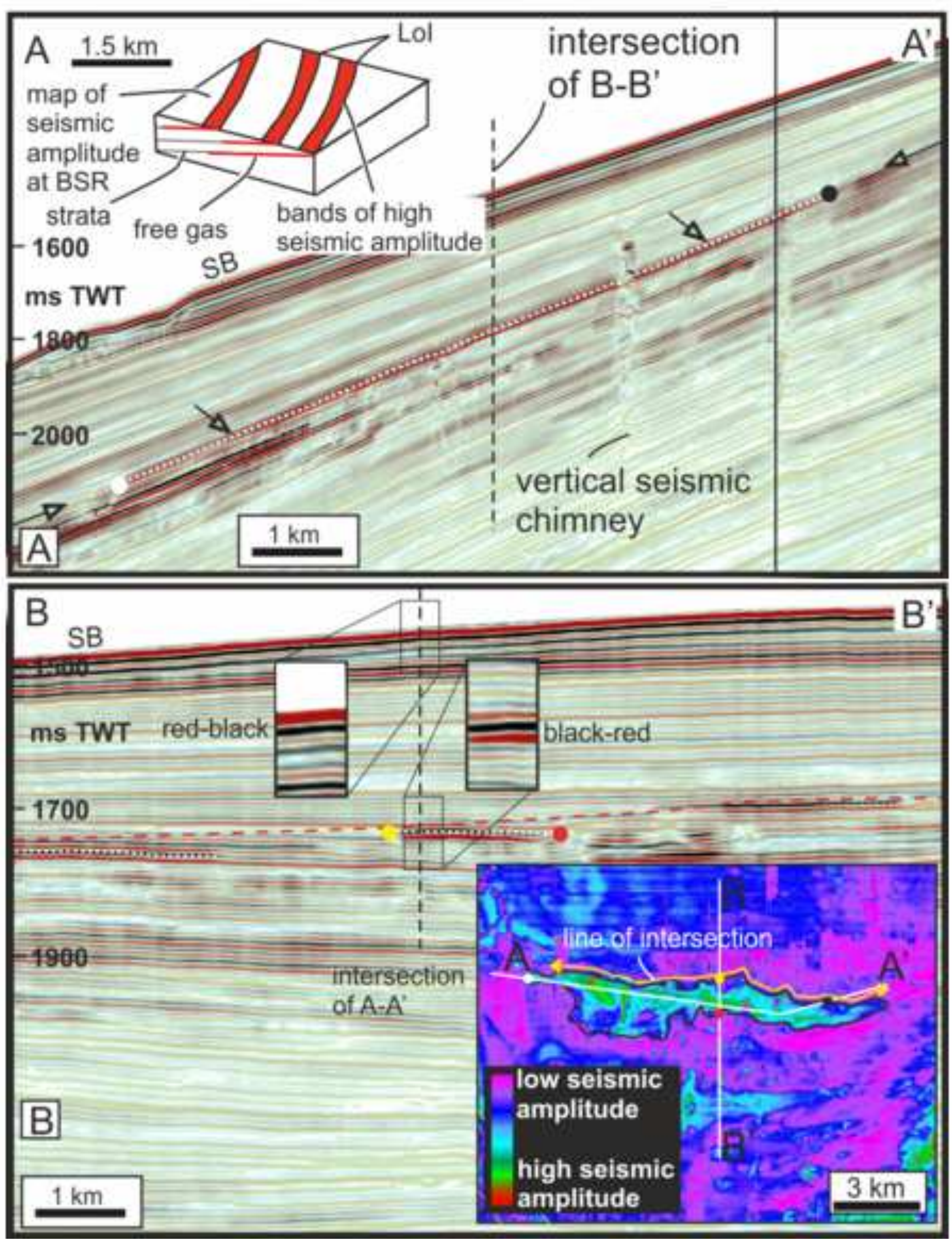

Figure
Click here to download high resolution image

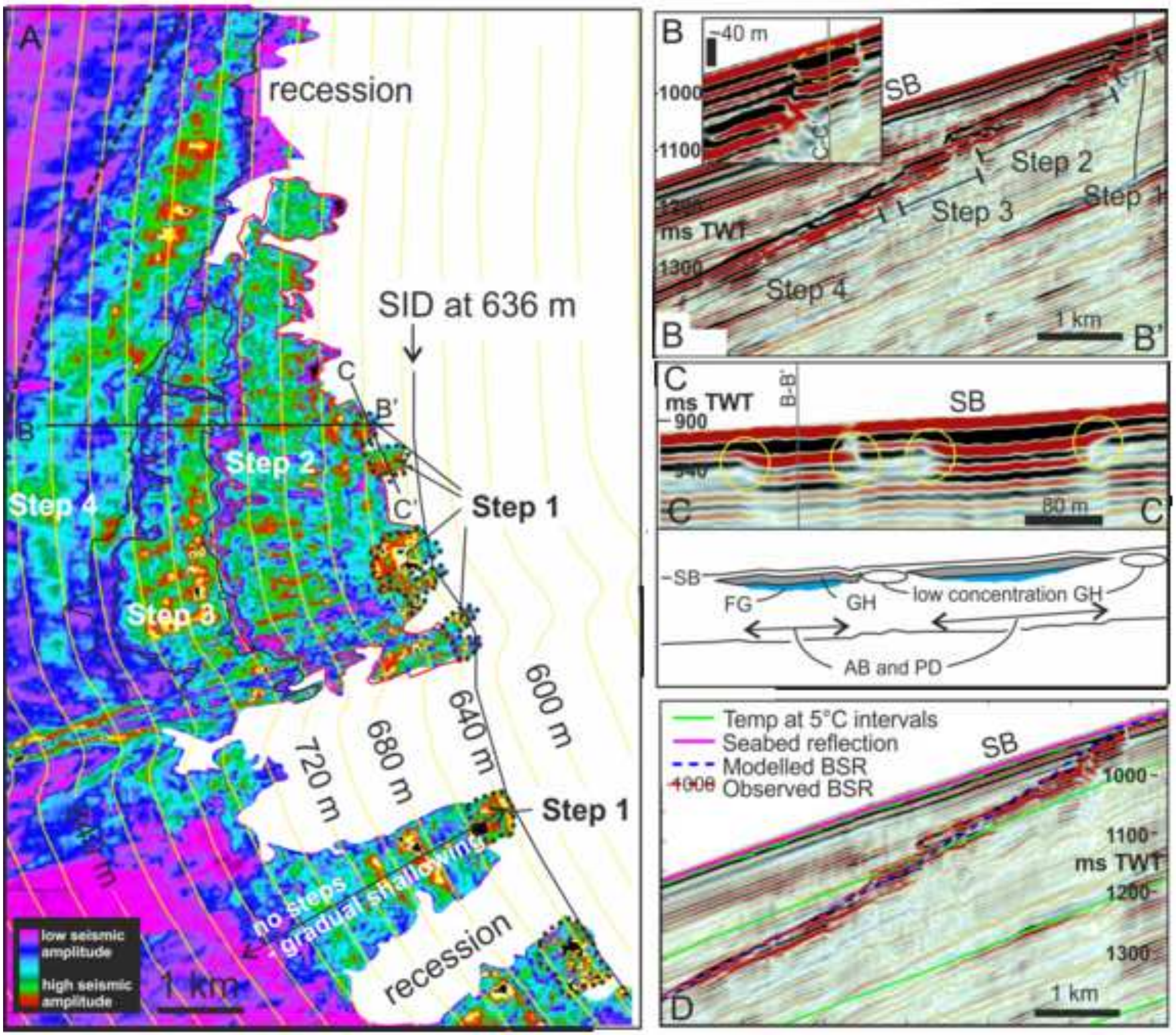

Figure
Click here to download high resolution image

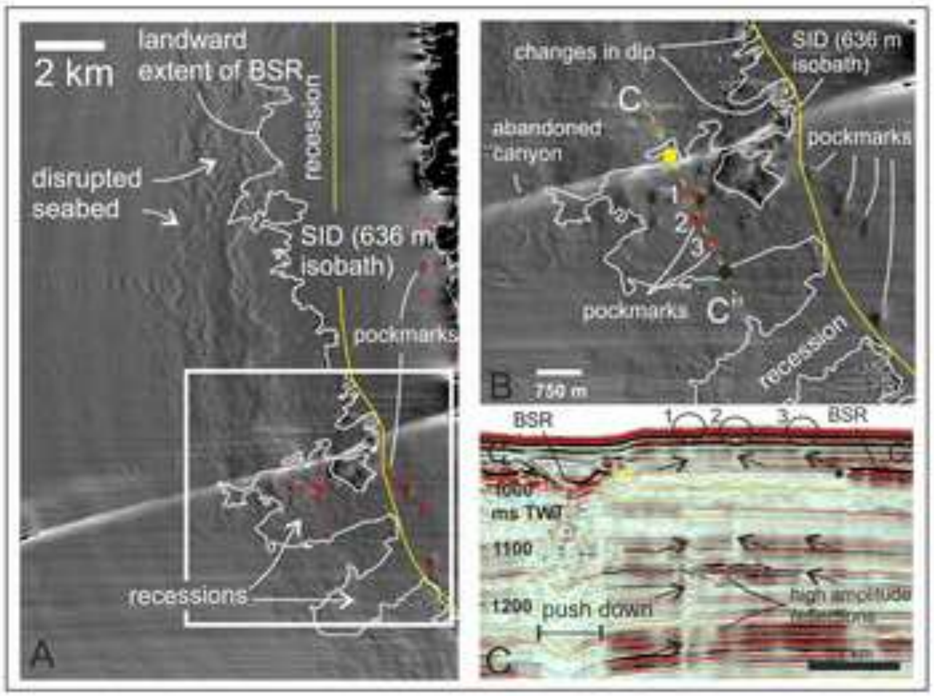

Figure
Click here to download high resolution image